Next Materials 11 (2026) 101741

Contents lists available at ScienceDirect

Next Materials

journal homepage: www.sciencedirect.com/journal/next-materials

Review article

Enhancing hydrogen storage in Mg alloys: Role of alloying, reinforcements, and severe plastic deformation techniques

Kavimani Vijayananth [a,b], Gopal Pudhupalayam Muthukutti [a,b], Sumsun Naher [c,*]

[a] Department of Mechanical Engineering, Karpagam Academy of Higher Education, Coimbatore, India
[b] Centre for Material Science, Karpagam Academy of Higher Education, Coimbatore, India
[c] Department of Engineering, School of Science and Technology, City St George's, University of London, London, EC1V 0HB, UK

ARTICLE INFO

Keywords:
Mg alloy
Alloying elements
Storage mechanism
Severe plastic deformation

ABSTRACT

Magnesium and its alloys have emerged as potential candidates for solid state storage of hydrogen owing to its higher theoretical capacity of ~7.6 wt%, abundance and lightweight nature. However, their practical application is hindered by slow hydrogenation kinetics, high thermal stability of hydrides and poor cycling performance. This review comprehensively discusses strategies to overcome these limitations that focusing on alloying, incorporation of catalytic reinforcements and the application of severe plastic deformation (SPD) techniques. Alloying with transition and rare-earth metals modifies thermodynamics and promotes reversible hydrogen storage while nanostructured reinforcements enhance diffusion pathways and catalytic activity. SPD techniques such as Friction Stir Processing (FSP), Accumulative roll bonding (ARB), Equal Channel Angular Pressing (ECAP), High Pressure Torsion (HPT), and cold rolling significantly refines the size of grain and also initiates lattice defects which accelerates the hydrogen sorption kinetics and improves structural stability. Synergistic effects of alloying, reinforcement and SPD are critically analysed along with their influence on thermodynamic destabilization and kinetic enhancement. The review also highlights the key challenges including process scalability, thermal management and long-term stability and also offers future perspectives to the fabrication of high-performance Mg based hydrogen storage systems.

1. Introduction

Evolution of next-generation materials has revolutionized the landscape of modern technology which enabled unprecedented advancements across diverse fields such as energy conversion and storage, flexible electronics, biomedical devices, aerospace systems and environmental remediation. These materials are designed with tailored structures sometimes at the nano or atomic scale exhibits superior mechanical, thermal, electrical or chemical functionalities that surpass conventional materials. The materials such as 2D materials, nanocomposites, metamaterials and High Entropy Alloys (HEAs) are the key next gen materials focused on modern applications. For example, 2D materials and nanocomposites are promising materials in developing high performance batteries and supercapacitors [1,2] whereas bio-inspired and stimuli-responsive polymers are reforming the targeted drug delivery and tissue engineering [3]. Similarly, lightweight HEAs, metamaterials and multifunctional ceramics are being explored for next-gen structural applications in extreme environments [4,5]. As demands for sustainability, efficiency and miniaturization continue to rise the integration of advanced materials into cutting-edge technologies becomes captious. Among these application areas, storage of hydrogen is one of the vital fields where development and deployment of advanced materials is vital to unlock its full potential [6].

The increase in demand for sustainable and cleaner energy technologies has intensified the worldwide research focus on hydrogen. It is a potential carrier of energy owing to its environmental friendliness and higher gravimetric energy density, e.g. lower heating value (LHV) of 33.3 $kWh \cdot kg^{-1}$ which is 12.4 $kWh \cdot kg^{-1}$ for gasoline and 13.9 $kWh \cdot kg^{-1}$ for natural gas [7,8]. However, the real time usage of hydrogen energy systems is critically limited by the lack of efficient, safe and compact hydrogen storage materials [9]. Hydrogen is currently stored in liquid form, compressed gas and solid state hydrides. The features such as comprehensive reversibility, higher gravimetric and volumetric hydrogen density, acceptable safety and option to work

* Corresponding author.
E-mail addresses: kavimani.s@kahedu.edu.in (K. Vijayananth), gopal.pm@kahedu.edu.in (G. Pudhupalayam Muthukutti), Sumsun.Naher.1@citystgeorges.ac.uk (S. Naher).

https://doi.org/10.1016/j.nxmate.2026.101741
Received 29 June 2025; Received in revised form 15 September 2025; Accepted 10 February 2026
Available online 25 February 2026

under ambient environments are ideal for a hydrogen storage method [10]. Though the compressed gas storage is the broadly followed method [11] for hydrogen it suffers from low volumetric energy density of 5.6 MJ·L^{-1} which is 32.0 MJ·L^{-1} for gasoline, high compression energy loss in the range of 13–18 % of the LHV [12], and the high cost of carbon fiber storage tanks. On the other hand, liquid hydrogen storage method necessitates deep cooling to −253 °C along with real-world liquefaction energy losses of 20–30 % [13] and boil-off losses of 1–2 % per day [14]. These drawbacks of gas and liquid storage methods make solid-state storage as an increasingly attractive alternative in which hydrogen is absorbed as atoms through chemical reaction to form metal, complex and chemical hydrides [15].

To store hydrogen atoms, lattice gaps of metals or alloys used for hydrogen storage serve as vacancies and forms metal hydrides (MH) [10]. Hydrogen is absorbed when the appropriate pressure and temperature condition is reached during which heat also produced. Since the reaction pathway for the majority of MHs are reversible, hydrogen desorption will take place once the temperature reaches the appropriate level. Rare earth, Magnesium (Mg), Titanium (Ti) and Vanadium (V) based MHs are the key research materials in this field at present [16–18]. Among various candidates, magnesium and its alloys have arisen as attractive solid-state hydrogen storage materials. This can be attributed to their high theoretical hydrogen capacity (~7.6 wt%), abundant availability, economical and lightweight nature. Mg based MHs are primarily based on MgH_2/Mg hydrogen sorption reaction, as shown in Eq. (1). The enthalpy change value of the reaction is about 75 kJ mol^{-1} H_2 [9,19,20].

$$Mg + H_2 \quad \leftrightarrow \quad MgH_2 \quad \Delta H \cong \quad \pm 75 \quad kJ\,mol^{-1}H_2 \tag{1}$$

Despite many advantages, the practical applicability of Mg based materials is constrained due to its slow sorption kinetics for hydrogen, higher thermal stability of hydrides and poor reversibility during cycling. Among this, higher thermodynamic stability and sluggish hydrogen absorption and desorption kinetics are the two dominating fundamental challenges that limits the application of MgH_2 as a hydrogen storage medium. The first hindrance is the high thermodynamic stability (ΔH = 74.7 kJ mol^{-1} H_2) resulting in the high decomposition temperature of MgH_2. The desorption enthalpy for MgH_2 should be tailored into the range of 42–55 kJ mol^{-1} H_2 for Mg/MgH_2 to release hydrogen near 1 bar and fuel-cell operating temperatures (50–150 °C) [21,22]. The second hindrance is the slightly sluggish hydrogen ab/de-sorption kinetics owing to slower rate hydrogen diffusion and high hydrogen dissociation energy barrier [9]. To overcome these limitations, various strategies have been explored, including alloy development using rare earth elements and transition metals incorporation of nano-structured reinforcements and application of severe plastic deformation (SPD) techniques.

Alloying can significantly alter the thermodynamic and kinetic behaviour of Mg by introducing catalytically active phases or destabilizing MgH_2 and thus the dehydrogenation temperature reduces and improves reversibility [23]. Similarly, the addition of nanostructured reinforcements such as metal oxides, carbides or carbon based materials enhance the hydrogen diffusion pathways and facilitates nucleation sites for hydride formation [24]. On the other hand, SPD techniques such as high-pressure torsion (HPT) and equal channel angular pressing (ECAP) are known to refine grain sizes to the nanoscale and consequently increasing grain boundary density and diffusion rates which play a pivotal role in improving hydrogen absorption/desorption rates [25]. Hence, this review aims to provide a comprehensive overview on the current research progress in enhancing the hydrogen storage performance in Mg-based systems through alloying, reinforcement strategies and SPD techniques. The microstructural evolution, thermodynamic tuning, kinetic improvements and synergetic effects of these approaches are deliberated in detail. The limitations and perspectives towards practical application of Mg alloys hydrogen storage materials are also critically discussed.

2. Hydrogen storage mechanisms of Mg and its alloys

Understanding the underlying mechanisms governing hydrogen desorption and absorption in Mg/MgH_2 system is essential for developing effective strategies to enhance the performance of Mg hydrides. This section provides a detailed analysis of the hydrogen storage behaviour of Mg alloys, focusing on the thermodynamic properties, kinetic barriers and cycling performance.

2.1. Thermodynamic properties and destabilization of the Mg/MgH_2 system

In order to evaluate the suitability for hydrogen storage, understanding the thermodynamic behaviour of the Mg/MgH_2 system is necessary. The hydrogenation of magnesium takes place along a multi-step mechanism. It starts with physisorption of hydrogen molecules on the metal surface through van der Waals forces followed by chemisorption in which molecular hydrogen dissociates into atoms and Mg–H bonding takes place. Then formation of a solid solution (α-phase) takes place as hydrogen atoms occupy interstitial sites and nucleation of the β-phase (MgH_2) begins once the hydrogen concentration reaches a critical threshold. Finally, the growth of the β-phase and disappearance of the α-phase thus completing hydrogenation.

These transformations are governed by pressure composition temperature (PCT) relationships as depicted in Fig. 1 [26]. From Fig. 1a., it can be observed that the hydrogen pressure, composition and temperature are the vital aspects that defines the phase equilibrium [27]. During isothermal hydrogenation, an initial increase in hydrogen pressure leads to solid solution formation. Once hydride nucleation begins the system exhibits a flat plateau region on the PCT curve where the β and α phases coexist. The plateau length represents the hydrogen capacity. As temperature increases, the plateau pressure rises and the length shortens. Above the critical temperature (T_c), the transition becomes continuous and no distinct plateau is observed.

The thermodynamic parameters of the system can be described by the van't Hoff Eq. (2) as

$$\ln P = \frac{\Delta H}{RT} - \frac{\Delta S}{R} \tag{2}$$

where R is gas constant (R = 8.314 J mol^{-1} K^{-1}), P denotes equilibrium pressure, T represent absolute temperature, ΔS and ΔH are the entropy and enthalpy of hydrogen absorption and desorption. The ΔS and ΔH can be obtained from the slope and intercept respectively. Especially, the de/re-hydrogenation enthalpy (ΔH) value is a chief indicator to quantify the Mg–H bond strength. The large absolute value of ΔH indicates the stronger Mg–H bond.

The thermodynamic stability of the Mg–H system is largely dictated by the strong covalent–ionic bonding character of Mg–H which exhibits a bond energy of ~3.35 eV. As a result, MgH_2 has a high decomposition enthalpy of ~74.7 kJ.mol^{-1} H_2 corresponding to the desorption temperature of ~280–300 °C at 1 atm. This value is significantly higher than the desired operating temperatures for practical applications such as on-board hydrogen storage. Numerous experimental studies have evaluated the thermodynamic properties of MgH_2 and reported ΔH values are typically in the range of 70–85 kJ.mol^{-1} H_2 and ΔS is from 119 to 146 J/mol·K depending on experimental conditions, sample purity and measurement methods. A study by Paskevicius et al. [28] confirmed a slightly lower ΔH (as low as ~71.2 kJ/mol H_2) for nanocrystalline MgH_2 (2–10 nm) compared to bulk which was attributed to the increased

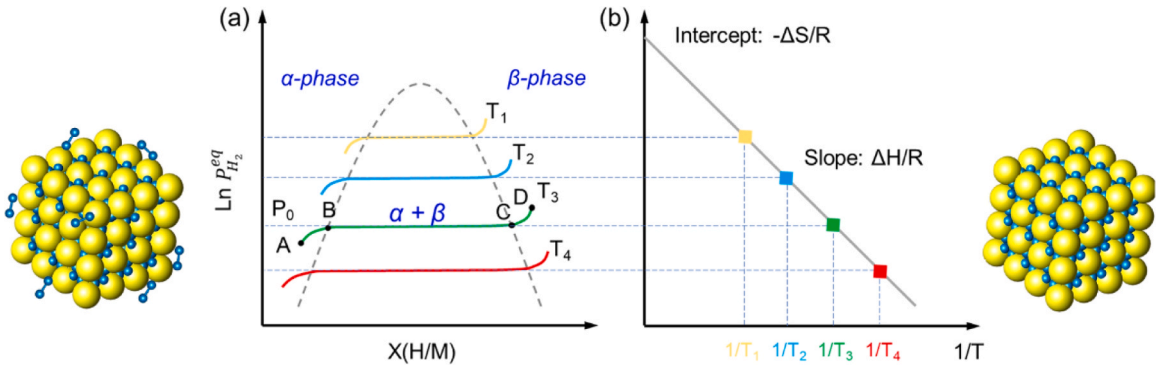

Fig. 1. (a-b) Pressure composition temperature and van't Hoff plot [26].

surface energy and transformed bonding environments. This confirms that the nanosizing of MgH_2 significantly influences its thermodynamics.

2.2. Hydrogenation and dehydrogenation behaviour

The real time use of MgH_2 in hydrogen storage depends on the kinetics of hydrogen desorption and absorption. Typically, Mg absorbs ~6.4 wt% H_2 at 363 °C under 22.7 bar in 1500 s and desorbs ~6.0 wt% H_2 at 390 °C under 1.5 bar in 500 s [29]. The reaction kinetics are governed by the activation energy (E_a) which can be determined using the Kissinger method or Arrhenius plots. Reported E_a values vary from 90 to 130 kJ/mol H_2 for absorption and 120–195 kJ/mol H_2 for desorption which is greatly influenced by the particle size, morphology and cycling [9]. For example, nano-sized MgH_2 (10–20 nm) shows a lower desorption E_a of 120 kJ/mol which is 156 kJ/mol for micro-sized particles (20 μm) [30].

The rate-limiting steps in hydrogen sorption are:

- Hydrogenation: diffusion through $MgO/Mg(OH)_2$ surface layers and the growing MgH_2 shell [31].
- Dehydrogenation: nucleation and growth of metallic Mg as shown by JMAK model fits [32].

Hydrogen diffusion barriers at the surface and subsurface of MgO layers are also significant (1.02–1.52 eV) in impacting overall kinetics. Models such as Jander (diffusion-controlled) and JMAK (nucleation-growth-controlled) effectively describe these processes.

2.3. Hydrogen storage kinetics

While thermodynamics dictates the feasibility of hydrogen storage the reaction kinetics determine its practical usability. In the Mg/MgH_2 system, hydrogenation follows four key steps: physisorption, H_2 dissociation, chemisorption and atomic diffusion [33] as depicted in Fig. 2. Each step presents an energy barrier with the rate-limiting step being hydrogen diffusion through the Mg lattice and MgH_2 layer [31]. Hydrogen diffusivity in Mg is low (~10^{-20} m^2/s in bulk and ~10^{-18} m^2/s along grain boundaries) [34,35]. Moreover, the initially formed MgH_2 shell hinders further hydrogen diffusion into the core which slowdowns the process [36]. In contrast, nano-sized MgH_2 particles facilitate uniform phase transformation and faster hydrogen movement thus improving desorption rates.

The kinetic behaviour is often modelled using the JMAK model (nucleation and growth mechanism), the shrinking core model (diffusion-limited) and the Arrhenius/Kissinger equations to derive activation energy (E_a) from reaction rate constants. Reported E_a values for hydrogen desorption vary typically ~160 kJ/mol H_2 for bulk MgH_2 which is significantly less for nanostructured systems. For example,

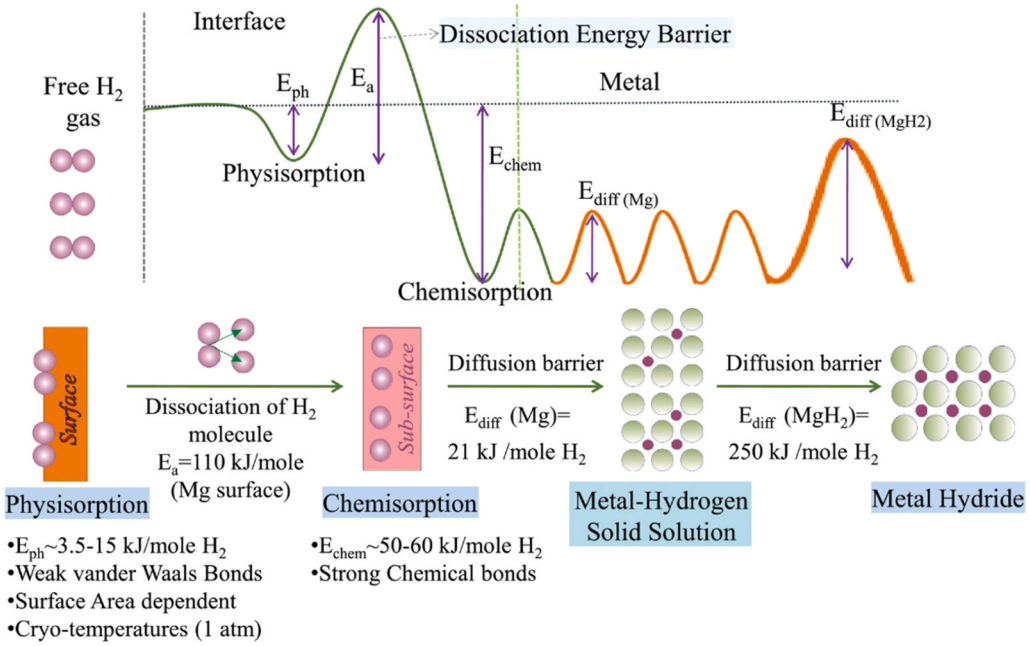

Fig. 2. Schematic illustration of hydrogen storage Mechanism [37].

nano-MgH_2 clusters (<19 atoms) exhibit dehydrogenation barriers below 1.5 eV even approaching negative desorption energies which indicates high instability and faster kinetics [38]. Ultimately, kinetic enhancement strategies including nano structuring, alloying and catalytic doping plays key role in making Mg-based hydrogen storage systems viable for real-world applications.

2.4. Cycling stability and structural degradation

The long-term usability of Mg-based systems is governed by their cycling stability i.e., the ability to maintain storage capacity and kinetics over multiple hydrogenation/dehydrogenation cycles. It is already proven that the hydrogen storage capacity and the hydrogen ab/desorption rate of these materials deteriorate over the time when used for long time at high temperatures [39]. The degradation of the Mg/MgH_2 system primarily arises from two factors: first, passivation at the Mg/MgH_2 interface due to reactions with impurity gases in hydrogen which reduces storage capacity [40]. Second, nanoparticle agglomeration and growth driven by interfacial energy increase the hydrogen diffusion path length thereby impairing kinetic performance. Apart from using purified H_2, the nanoconfinement and encapsulation strategy are found effective for hindering the agglomeration and growth of nanoparticles in view of maintaining cyclic stability.

Structural degradation is a main problem associated with Mg based materials when used in hydrogen storage applications. Magnesium-based materials are prone to particle coarsening and sintering which reduce surface area [36]. Also, surface oxidation led to formation of MgO or $Mg(OH)_2$ [41]. Protective coatings, structural reinforcement using stable matrices, and carefully engineered alloy compositions have been employed to mitigate these issues. For example, carbon coatings or TiO_2 shells can preserve activity and resist oxidation while carbon matrices help to maintain dispersion and suppress sintering.

2.5. Influence of impurities in storage performance

Magnesium and its hydride (MgH_2) are highly sensitive to oxygen and moisture which negatively affect their hydrogen storage performance. Upon air exposure, Mg rapidly forms MgO and $Mg(OH)_2$ surface layers which act as barriers to hydrogen diffusion and surface activation. Even trace amounts of O_2 or H_2O will lead to irreversible deactivation and capacity loss during cycling [42]. It was reported that the Mg powder exposed to just 0.5 % O_2 experiences ~ 20 % permanent loss of initial capacity. Conversely, a small amount of MgO can enhance hydrogen absorption and desorption kinetics through catalytic effects [43,44]. For example, Hjort et al. [43]observed that Mg films exposed to a low oxygen dose (150 $ng{\cdot}cm^{-2}$) showed improved H_2 uptake rates, whereas higher oxygen exposure led to slower absorption due to the formation of a thick oxide layer. On the other hand, in kinetics of MgH_2 systems, N_2 exhibit negligible effect in hydrogenation and dehydrogenation. N_2 will not form MgO and also it will increase crystallization unlike O_2. Larger particle sizes may increase activation energy, but N_2 itself does not alter adsorption/desorption behaviour [45]. Fei Sun et al. [46] observed that in the presence 1 mol.% N_2 or CH_4, MgH_2 system with $2LiNH_2$ exhibits stable hydrogen storage. However, presence of 0.1 mol.% O_2 leads to the formation of $LiNH_2$ and MgO, that decrease the hydrogen capacity from ~5 wt% to 4.41 wt% after multiple cycles. This fact increases dehydrogenation and reduces desorption kinetics. Presence of lower N_2 impurities (0.5 mol.%) can inhibit hydriding in pure Mg_2Ni, while Na-modified Mg–Ni alloys resist up to 5 mol.% N_2. Hydrogen absorption follows a nucleation growth mechanism, with higher N_2 decreases the hydriding and increasing the activation energy. Addition of Na in Mg–Ni surface adsorbs N_2 selectively and leaves metallic Ni available for H_2 dissociation and activated hypoeutectic alloys that show higher kinetics than as-cast alloy [47]. Moreover, oxide and hydroxide layers increases the activation energy for hydrogen diffusion and requires higher temperatures to overcome. These layers are responsible for the long incubation period before hydrogen absorption begins especially in untreated or aged samples. To mitigate these effects, several strategies like protective coatings (e.g., carbon, metal oxides, polymers) to isolate Mg from air and moisture, inert atmosphere processing and storage, core–shell nanostructures where Mg is encapsulated within stable, hydrogen-permeable shells are used. Ultimately, controlling surface oxidation and environmental exposure is essential for maintaining reversibility and capacity in Mg-based hydrogen storage systems.

3. Effect of various alloying elements and reinforcement

A variety of strategies have been investigated to overcome the limitations of Mg in hydrogen storage such as slow hydrogen absorption/desorption kinetics and high thermodynamic stability, which requires elevated temperatures for hydrogen release. Among that the alloying and reinforcement are two of the most effective approaches. Various alloying elements especially transition metals (TMs), p-block elements and rare-earth (RE) elements along with reinforcements are explored for enhancing the hydrogen storage performance of Mg.

Alloying alters the bonding environment around hydrogen atoms which modifies the thermodynamics of hydrogen storage. For example, Ni and Al addition reduces the desorption enthalpy (ΔH) that enables lower operating temperatures. The alloying can reduce ΔH from ~74.1 kJ/mol to ~55–65 kJ/mol depending on the alloying system. Kinetically, the activation energy (Ea) for hydrogen desorption can be lowered from above 150 kJ/mol (in pure MgH_2) to as low as 45–70 kJ/mol in properly alloyed systems [48]. Alloying has greater influence on microstructural aspects such as grain refinement, lattice strain and defect formation which plays key role in enabling hydrogen diffusion and enhancing the rate of absorption/desorption. Nano alloyed systems like $Mg_2Ni_{0.8}Mn_{0.2}$ prepared by high-energy ball milling (Fig. 3) showed hydrogen uptake within 1.5 mins with the storage capacity of 3.7 wt% which clearly validates the kinetic advantage of tailored compositions [49].

Alloying magnesium with p-block elements such as silicon (Si), germanium (Ge), tin (Sn) and aluminum (Al) significantly influences the thermodynamic and kinetic parameters of hydrogen sorption. These elements have tendency to form intermetallic phases with Mg thereby altering the hydrogen diffusion pathways, destabilizing MgH_2 and ultimately reducing desorption temperatures. For example, Si, Ge and Sn form compounds such as Mg_2Si, Mg_2Ge and Mg_2Sn through reactions with MgH_2 releasing hydrogen as a byproduct. The associated reaction enthalpies are 36.4 kJ/mol H_2 for Mg_2Si, 14 kJ/mol H_2 for Mg_2Ge and 44.5 kJ/mol H_2 for Mg_2Sn [50–52]. These values are significantly lower than the standard enthalpy of MgH_2 (74.1 kJ/mol H_2) which indicates the favourable thermodynamic destabilization. Moreover, their hydrogen release capacities at elevated temperatures (~350°C) range from 2.4 to 5.0 wt% that shows the potential for practical use. Among the p-block elements, aluminium is particularly notable due to its dual role in enhancing kinetics and improving oxidation resistance. Al addition results in the formation of $Mg_{17}Al_{12}$ and Mg_2Al_3 phases [53] which act as catalysts during dehydrogenation. Furthermore, studies confirmed that the Al substitution reduces the desorption activation energy from 100 kJ/mol [31] to as low as 56 kJ/mol [53]. This improvement is attributed to the shortened diffusion paths, inhibition of Mg particle agglomeration and enhanced nucleation kinetics. For example, Zhong et al. [53] reported that an alloy with 10 mol.% Al absorbed 5.5 wt% hydrogen in just 600 s and showed 6 wt% total storage under 20 bar H_2 pressure.

Transition metals (TMs) like nickel (Ni), copper (Cu), cobalt (Co), titanium (Ti), palladium (Pd), iron (Fe) and zinc (Zn) form a broad class of magnesium alloys that demonstrate improved hydrogen storage behaviour through both catalytic and structural effects. Mg_2Ni is one of the most extensively studied magnesium-transition metal hydride [54]. The hydrogenation of Mg_2Ni forms Mg_2NiH_4 with a dehydrogenation

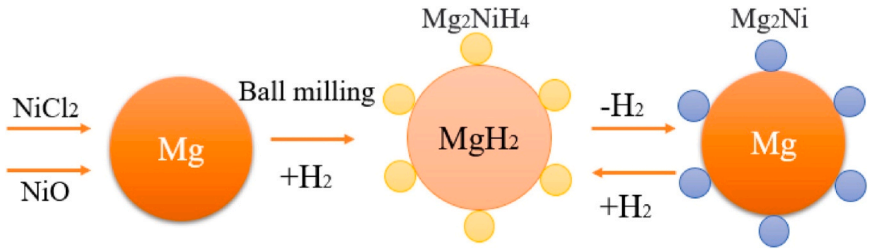

Fig. 3. Representation of intermetallic formation in Mg-Ni alloy system [48].

enthalpy of ~64.4 kJ/mol H_2 [55] which is lower than MgH_2 and it resulting in reduced equilibrium temperatures (~240°C at 1 bar H_2) [56]. Though the gravimetric hydrogen capacity decreases to ~3.53 wt % [55], this trade-off is compensated by its superior reversibility and kinetic performance. Hydrogen storage properties od various Mg alloy are depicted in Table 1.

The Mg_2Cu system undergoes a reaction yielding MgH_2 and $MgCu_2$ with an associated enthalpy of ~72.8 kJ/mol H_2 [58]. While its capacity (~2.53 wt%) is lower than MgH_2, the reaction occurs more rapidly due to the enhanced electron transfer and phase transformations particularly when the alloy is nanostructured. Mg_2CoH_5 and Mg_2FeH_6 are other hydride-forming compounds with practical interest. Mg_2FeH_6 offers 5.5 wt% hydrogen capacity and high volumetric density (~150 kg H_2/m^3) [59]. Its desorption is facilitated due to a bi-phase nature (β-MgH_2 + Mg_2FeH_6) that results in faster hydrogen release kinetics. Pd-containing systems such as Mg_6Pd demonstrate reversible transformations that enables capacities around 3.96 wt% [60]. Similarly, Ti forms stable intermetallics with Mg which can destabilize MgH_2 thermodynamically and enhance its catalytic activity in hydrogenation reactions thermodynamic behaviour various Mg alloys are provided in Table 2.

Rare earth elements (La, Pr, Nd) have been successfully alloyed with Mg and Ni to create multi-phase intermetallics classified as AB_2, AB_3 and A_2B_7 types. These compounds exhibit favourable structural motifs (e.g., Laves phases) which as favourable to hydrogen storage. For example, AB_2-type compounds like $La_{1-x}Mg_xNi_2$ retains C15-type structure when Mg replaces La up to a critical ratio [61]. These alloys showed improved kinetics and altered thermodynamics due to the structural transformation from anisotropic to isotropic hydrides. AB_3 and A_2B_7 compounds demonstrate a linear relationship between Mg content and hydrogen equilibrium pressure which confirms that tuning crystal structure can directly influence desorption enthalpy and hydrogen release pressure [48].

Table 1
Various Mg alloy with respective hydrogen storage properties [57].

Mg Alloy	Elements	Storage Capacity of Hydrogen (wt %)	Desorption Temp. (°C)	Hydrogen Kinetics
Mg-Ce	Mg-30 wt% Ce-10 wt% Co	4.6	260–300	RF
	Mg-30 wt% Ce	4.8	270–320	M
Mg-Ni	$Mg_2Ni_{0.7}Mn_{0.3}$	3.5	240–290	RF
	$Mg_2Ni_{0.8}Co_{0.2}$	3.4	270–320	F
	Mg_2Ni	3.6	250–300	M
Mg-Co	Mg_2CoH_5	4.5	280–320	M
Mg-Ti	Mg-10 wt% Ti	6.0	250–300	F
	Mg-5 wt% Ti	6.8	300–340	F
	Mg-5 wt% Ti-5 wt% Fe	5.5	240–280	VF
Mg-Fe	Mg-10 wt% Fe	6.2	330–360	RS
	Mg_2FeH_6	5.5	320–350	S
Mg-La	Mg-30 wt% La-10 wt% Ni	4.8	230–280	VF
	Mg-30 wt% La	5.0	250–300	F
Mg-V	Mg-5 wt% V-5 wt% Ni	5.8	190–240	F
	Mg-10 wt% V	6.5	200–250	EF

F- Fast; M- Moderate; Relatively Fast- RF; Relatively slow- RS; Slow- S; Extremely fast- EF

Table 2
Thermal kinetics of Mg alloys [57].

Alloy System	Enthalpy ΔH (kJ/mol H_2)	Entropy ΔS (kJ/(mol·K))	Desorption Temperature (°C)
Mg-Ni	64.5	130.2	255
	62.8	126.5	246
	65.9	132.6	262
Mg-Fe	77.4	137.8	320
	75.6	135.2	311
	79.1	140.1	326
Mg-Co	75.1	135.5	310
	73.5	132.8	301
	76.4	137.3	318
Mg-Ti	72.3	133.1	288
	70.7	130.6	280
	73.5	135.0	295
Mg-Nb	68.7	132.4	275
	67.4	129.8	267
	70.2	134.6	282

In addition to metallic alloying, the inclusion of catalytic reinforcements such as metal oxides (e.g., Nb_2O_5, TiO_2), carbon nanotubes (CNTs), graphene and metal-organic frameworks (MOFs) has become a prominent approach to enhance Mg-based hydrogen storage. For example, the addition of Ni/TCN composites reduces the activation energy from 161.1 kJ/mol to 82.6 kJ/mol and also enhances the cycling stability [62]. Added TCN served as both a catalyst and a physical framework which prevented agglomeration and enhanced hydrogen diffusion pathways. Similarly, Ni@Pt core-shell structures reduced the desorption temperature of MgH_2 by more than 100 K [63] which indicates the potential of surface engineering strategies. High-entropy and medium-entropy alloys (HEAs/MEAs) such as FeCoNiCrMn and $Ti_{0.35}V_{0.35}Nb_{0.2}Cr_{0.1}$ are also employed as reinforcements. These complex systems offer combination of lattice distortion and multiple catalytic centres which synergistically reduces the hydrogen diffusion barriers. Doping MgH_2 with HEAs showed reductions in activation energy by 40–50 % and considerable enhancement in the desorption rate.

Addition of bimetallic carbide such as $Ni_3ZnC_{0.7}$/Ni@CNT in MgH_2 forms intermetallic such as Mg_2Ni and Mg_2NiH_4 that provides more channels for hydrogen diffusion [18]. Similarly, the presence of $MgZn_2$ and Zn form nucleation sites to suppress MgO and decrease the agglomeration which increases the H_2 diffusion, dissociation and cycling stability as depicted in Fig. 4. Likewise, Ti and Nb has ability to form carbides/MXenes and oxides on MgH_2 that improves the hydrogen storage performance. When Nb and Ti oxides reacts with MgH_2 it produces mixed-valence of Mg-TM-O complexes that create whole in MgO layer. It acts as carrier for transfer of electron among H^- and Mg^{2+} that increase the absorption and desorption of hydrogen. Further formation of oxide decomposition act as the active catalytic that accelerate the reaction kinetics. Addition of MXenes and carbide in MgH_2 provides

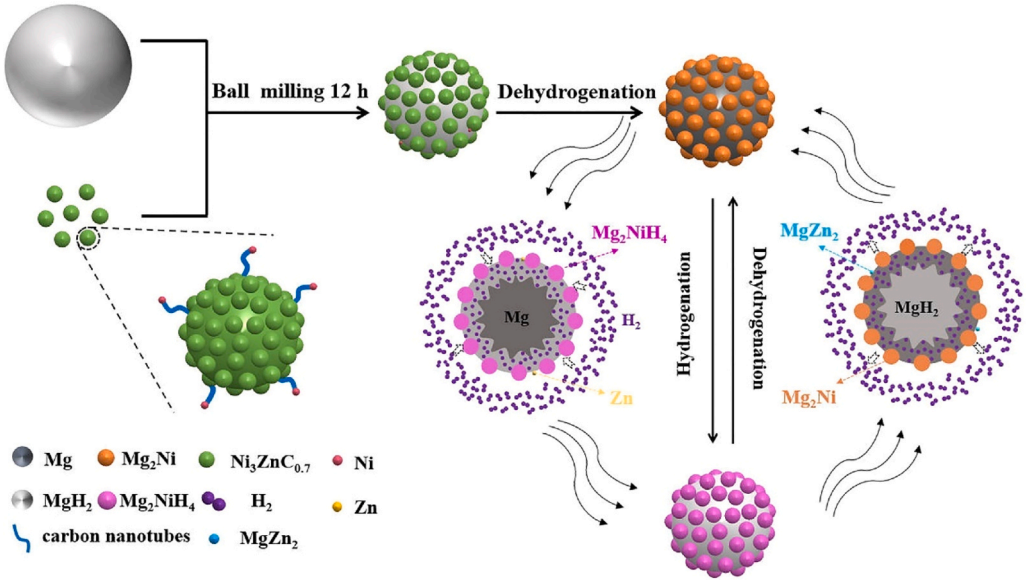

Fig. 4. Catalytic mechanism in MgH_2 system [18].

hydrogen diffusion pathways due to its layered structures and decrease the chance of agglomeration during cycling [64].

4. Severe plastic deformation Mg and alloys

Numerous researches have been reported on severe plastic deformation of Mg alloy to improve the mechanical properties for structural applications [65,66]. SPD methods alter the texture, increases dislocation density and initiates grain refinement that increase the mechanical strength of Mg alloys [67,68]. Rolling, High-Pressure Torsion (HPT) [69], Equal Channel Angular Pressing (ECAP) [70], friction stir processing (FSP) [71] are some of the common SPD methods for Mg alloy. Herein strain is applied in Mg alloy on both hot and cold condition in rolling approach to attain fine grain refinement. Strain is induced under high pressure and repeated discontinues strains reapplied in case of high-pressure torsion and ECAP method to achieve refinement in grains. However, research work related to SPD for hydrogen storage application are limited. These SPD approaches can also be used for enhancing storage performance of Mg and its alloys.

4.1. Equal channel angular pressing

Among available SPD process, ECAP process is the earliest method identified to significantly improves the hydrogenation kinetics of Mg alloys [72]. In this method, Mg alloy is taken in the form of billet or rod and it is pressed repeatedly through a channel having bending angle to apply shear strain. This repeated pressing results in reduction of grain size from micron to submicron levels. These billets are also processed through different routes based the rotation of sample. In ECAP, route A represent the pressing of sample without rotation, pressing sample at 90 ° rotations in between the passes at same direction is termed as route B and sample pressing at 180 ° is named as route C [73]. Song-Jeng Huang et al., [74] adopted B_C route in ECAP process to improve the hydrogen storage behaviour of AZ61 alloy. It was observed that increase in number of passes results in formation of $Mg_{17}Al_{12}$ precipitates which act as catalytic sites that improves the hydrogen absorption capability and attained 6.2 wt% hydrogen storage at 8th pass. ECAP on Mg, AZ31 and ZK60 alloy also generated basal plane sliding that increases the density of twins and dislocation density which increases kinetics of hydrogen sorption [75]. ECAP process reduces the activation time and increases the absorption and desperation rate in various Mg alloy system that includes Mg- Ni alloy [76]. In addition to faster kinetics, ECAP shown decrease in activation energy for hydrogen release, that effectively alters the hydrogenation and dehydrogenation processes to lower temperatures. Recent studies combining ECAP with low-temperature rolling further confirmed that these microstructural changes improve absorption/desorption kinetics and allow operation at comparatively lower temperatures [77]. ECAP process induce grain reinforcement and crystallographic defects that increase the surface area and vacancy density in Mg alloy that improve hydrogen storage. Likewise, it induces texture orientation and grain boundaries that favours hydrogen diffusion [78]. ECAP process is also coupled with other processing technique such as ball milling and rolling process to improve the hydrogen storage of Mg. Alberto Moreira Jorge et al. [79] performed cold rolling process on ECAP processed AM60D and AZ91 alloy. It was observed that cold rolling forms the (0001) texture and form different amounts of precipitates in alloys. The texture acts synergistically with grain size that increase the hydrogen sorption properties. Formation of intense texture are 18 time the random value for AZ91 alloy whereas AM60 D alloy has only 13 times the random values (Fig. 5a-b). These textures influence the hydrogenation kinetics of the alloys in achieving their full storage capacity. For example, AZ91 alloy has a hydrogen capacity of 4.6 wt% and takes 15 h to reach it whereas the AM60D alloy with a capacity of 6.2 wt % requires 40 h to attain full absorption.

Juliano Soyama and coworkers [80] combined melt spinning, ECAP and cold rolling process to improve hydrogen storage capacity of ZK60 alloy. Initially, the ingot is processed by melt spinning method for ECAP and cold rolling processing. It was observed that cold rolling breaks down the intermetallic network form on the grain boundaries as the after effect of ECAP. Herein cold rolled ECAP processed alloy exhibit 4 wt% and cold rolled alloy developed by melt spinning process showcase 4.5 wt% storage capacity. The same alloy was processed with ECAP and accumulative roll bonding by A.A.C. Asselli et al. [81] to improve its hydrogen storage properties. Initially, ZK60 alloy extruded into road then processed through ECAP followed by accumulative roll bonding. It was depicted that combination of ECAP and ARB process limits the storage capacity of alloy viz. less than 4 wt% due to low surfaces to volume ratio. Also found that pulverization of developed samples increases the kinetic and hydrogen storge capacity. Researchers also used various additives in Mg alloy and adopted ECAP process to improve the performance. Carbon black and graphene use used as reinforcement in AZ31 alloy. The developed samples are processed with ECAP technique then filed and milled using high energy ball billing by Song-Jeng Huang et. al. [82]. The processed carbon black-reinforced Mg alloy shown a

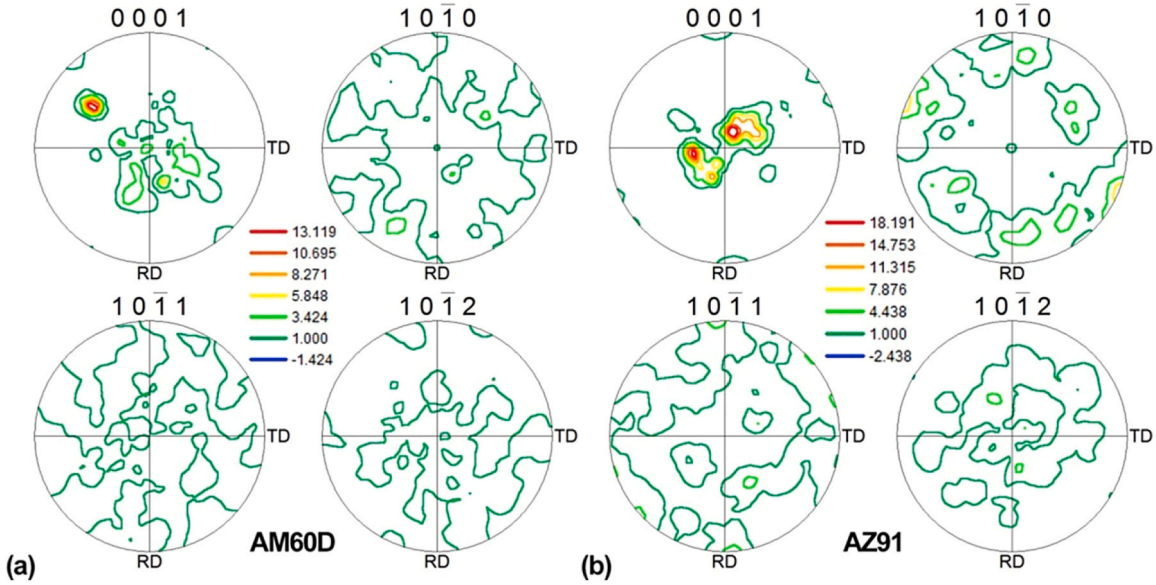

Fig. 5. ECAP and cold rolled pole figure of a) AM60D Mg alloy (b) AZ91 Mg alloy [79].

higher hydrogen storage capacity of 6.72 wt% whereas the graphene-reinforced composite achieved a slightly higher capacity of 6.83 wt%. The full capacity is attained within 792 s, with the onset of hydrogen uptake observed at 143.2 s. The proposed absorption/desorption mechanism of hydrogen is depicted in Fig. 6. During hydrogen uptake, H_2 molecules dissociate and diffuse into the Mg matrix to form MgH_2 whereas MgH_2 decomposes back into Mg and H_2 during release under suitable thermal and pressure conditions.

The same research team investigated the effect of varying nickel content in AZ31 alloy using both ECAP and HEBM processing techniques [83]. Results revealed that the ECAP-processed AZ31 alloy with 4 wt% nickel exhibited the highest hydrogen storage capacity of 7 wt% and complete desorption achieved in 2322 s. This enhancement is attributed to the ECAP process which promoted the dissolution of AlNi and the formation of Mg_2Ni/Mg_2NiH_4 phases; additionally, the ECAPed alloy demonstrated a lower activation energy for desorption, thereby improving overall hydrogen storage performance. The ECAP process was also applied to AZ61 alloy composites reinforced with SiC and Ni fillers. The composite containing 1 wt% SiC exhibited a hydrogen storage capacity of 6.8 wt%. However, the addition of 1 wt% Ni reduced the capacity to 6.5 wt%. ECAP induces the formation of secondary phases such as β-$Mg_{17}Al_{12}$, Mg_2Si and Al_3Ni, which act as catalytic sites and enhanced hydrogen storage performance. Conversely, the addition of Ni promotes the formation of Mg_2Ni which has lower storage capacity but better kinetics, ultimately resulting in a slight reduction in overall hydrogen storage capacity [84]. Aqeel Abbas et al. [85]used graphene, CNTs and organic additives in ZK60 alloy processed through ECAP. It was observed that the addition of CNTs and graphene increased the hydrogen storage capacity up to 7.21 wt% and 7.28 wt%, respectively. The study demonstrated that these nanofillers exhibits a catalytic effect thereby reducing activation energy and providing a high surface area that promotes rapid hydrogen diffusion.

4.2. *High pressure torsion*

HPT method involves applying a high shear strain to the bulk volume of the sample by subjecting it to uniaxial pressure combined with torsional strain, with the sample positioned between two anvils. Application of this method in Mg based metal hydrides improves grain refinement and form (002) texture that improves hydrogen storage capacity of Mg [86]. HPT process on pure Mg exhibits 6.9 wt% hydrogen absorption after 10 revolutions. It induces ultrafine grain refinement that accelerates hydrogen kinetics and increases the fraction of high-angle grain boundaries which serve as diffusion pathways for hydrogen [87]. HPT process is also used to process Mg-Zr alloy that form metastable phases (nano-twinned FCC) that store hydrogen reversibly.

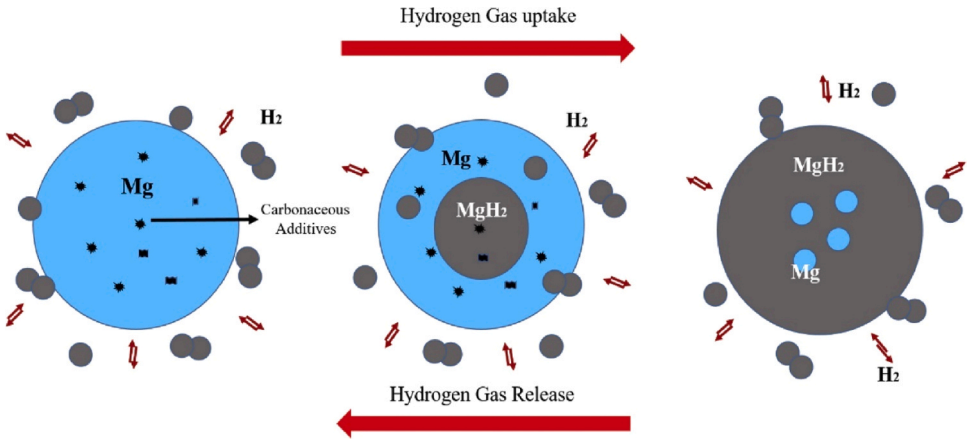

Fig. 6. Graphical representation of hydrogen kinetics of Mg alloy [82].

HPT process enhances the hydrogen storage by generating high grain boundary density and significant grain refinement that enables the absorption of 1 wt% hydrogen within 20 s and its rapid desorption at room temperature [88]. HPT process on Mg–Ti alloy forms metastable phases with FCC, BCC and HCP structures. Formation of these phases enhance the storage performance of alloy [89]. In the case of Mg_2Ni intermetallic, HPT reveals stacking faults and grain boundary which act as activation sites for enhanced absorption performance [90]. Subrata Panda et al. observed that HPT processing of Mg powder enhances hydrogen kinetics due to oxide dispersion and grain refinement. It was also reported that ultrafine powder exhibited lower hydrogen storage capacity because of the presence of MgO whereas the atomized powder showed rapid desorption behaviour with lower activation energy [91]. Amorphous Mg65Ce10Ni20Cu5 alloy are also processed using melt spin method and treated with HPT to improve it hydrogenation kinetics. Enhanced hydrogenation kinetics was observed for Mg alloys by generating nano glass regions and interfaces that act as rapid hydrogen diffusion pathways. Among the treated samples, the 1-turn HPT alloy exhibited superior kinetics and capacity due to its optimal balance between structural stability and amorphous fraction [92]. M. Osorio-García et al. [93] demonstrated that HPT of Mg-5Ni-2Nb_2O_5 alloys yields ultrafine-grained materials with enhanced air stability and hydrogenation kinetics. However, moderate hydrogen storage capacity of ~5.5 wt % was attained owing to MgO formation and the materials exhibits fast kinetics. It was also depicted that catalytic effect of Ni and formation of Mg_2NiH_4 are played major role for its improved performance. A. Revesz and coworkers observed that HPT process enhances hydrogen absorption in amorphous $Mg_{65}Ni_{20}Cu_5Y_{10}$ alloys by inducing deformation-dependent microstructure with dispersed Mg_2Ni nanocrystals. The hydrogen uptake shifts to lower temperatures at ~390 K and increases nearly threefold after HPT due to the additional hydrogen sorption sites at amorphous nanocrystal interfaces. HPT process is also combined with other SPD methods to improve the storage capacity. Andreas Grill et al. [94]performed cold rolling process on HPT processed ZK60 alloy and also with Mg hydride. It was observed that ZK60 alloy depicts faster kinetics and long-term stability due to the thermally stable SPD induced defects. However, slower kinetics and capacity loss are observed for Mg metal hydrides. Johnson Mehl Avrami Kolmogorov (JMAK) theory depicts that for ZK60 alloy, cold rolling forms only nucleation and presence of Zn, Zr contribute to improved storage performance. While nucleation and growth are taking place in metal hydrides that dominantly blocks the hydrogen diffusion. P. Cengeri et al. [95] compared the effect of HPT and FSP over ZK60 alloy on hydrogen storage performance. It was observed that FSP treated alloy exhibits 30 % better storage capacity than HPT processed alloy. The improved performance is attributed to higher density thermally stable vacancy agglomerates that act as effective nucleation sites for hydride formation. For both the SPD methods, JMAK analysis shows shift from homogeneous to heterogeneous nucleation that indicates defect driven hydride growth that ensures consistent hydrogen storage. It was found that FSP form more slip systems which leads to enhanced defect density and superior microstructural conditions when compared with HPT. HEBM was also used with HPT to develop Mg-Nb_2O_5-CNT composite with improved hydrogen storage performance. It was observed that the combined process induces (002) texture that improves the sorption kinetics and hydrogen diffusion [96]. Addition of Nb_2O_5 and CNT act as the catalyst to form nucleation sites and stabilize the microstructure near grain boundaries that facilitate hydrogen transport. HPT on developed composite promotes synergistic effect and interaction between Nb_2O_5 and CNT that improves hydrogen release kinetics. The potential of HPT strategy lies in its ability to induce ultrafine grain refinement, increase high-angle grain boundary density and form metastable phases that serve as fast hydrogen diffusion pathways. This leads to improved hydrogen storage capacity, accelerated absorption/-desorption kinetics and better cycling stability. Furthermore, the combination of HPT with alloying elements and catalytic additions has shown synergistic effects, decreased activation energy and enhanced kinetics. These features make HPT a promising SPD approach for tailoring Mg-based hydrogen storage materials for practical applications.

4.3. Rolling

In Mg and its alloys, rolling induces 002 texture that enhances hydrogen sorption kinetics by promoting diffusion pathways. Further it reduces the incubation time and faster hydrogenation/dehydrogenation by promoting finer grain refinement and catalytic secondary phases. S. Amira and J. Huot [97] performed cold rolling on AZ91D, MRI153, AXJ530 and ZAEX10430 alloy to understand its effect on hydrogen storage capacity. It was observed that cold rolling promotes grain refinement and increases defect density which accelerates hydrogen diffusion and improves sorption kinetics. Furthermore, it decreases the incubation time for hydrogen absorption for AZ91D and MRI153. Among them, AXJ530 showed poor performance due to the formation of coarse precipitates. Rolling is also performed in Mg-Cu and Mg-Pd laminates that forms dense dislocations and vacancies, enhancing hydrogen diffusion and reaction kinetics. For Mg-Cu composites, distinct Mg and Cu layers with dense lattice defects with intermetallic phases formed during the initial activation process contributed to hydrogen storage performance. The processed Mg-Cu composites showed improved kinetics and reversibility compared to melt-cast Mg_2Cu alloys, aided by the unique lamellar structure and retained defects after activation. For Mg-Pd composites, reversible hydrogen absorption and desorption occurred through disproportionation and recombination, forming MgH_2 and MgPd, with maximum hydrogen content of ~1.47H/M [98,99]. José J. Márquez et al. [100] performed cold rolling on MgH_2 to investigate its effect on hydrogen storage performance. It was observed that cold rolling significantly reduces particle size and achieved optimal hydrogen kinetics after 35 passes. The study also suggested that cold rolling is a promising alternative to ball milling for producing nanostructured MgH_2. The MgH_2–$LaNi_5$ composite was developed using a cold rolling approach which promoted the formation of a nanocrystalline structure and the emergence of Mg_2NiH_4 and LaH_3 phases after cycling. These intermediate hydrides plays a crucial catalytic role in enhancing the hydrogen storage kinetics of MgH_2 [101]. Various additives such as Fe, Nb, Fe_2O_3, Nb_2O_5 and FeF_3 were also incorporated into MgH_2 and processed via cold rolling. The results revealed that cold rolling produces nanostructured materials with crystallite sizes ranging from 8 to 17 nm. Among the additives, FeF_3 and Nb_2O_5 showed a significant enhancement in hydrogen desorption kinetics at lower temperatures [102].

ARB process is also used to improve the hydrogen storage in Mg alloy which forms ultra fine grain refinement by repeated cold rolling and folding of Mg alloy. Mohsen Danaie et al. [103]adopted ARB process for Mg-Ti and Mg-SS multilayer composite. It was observed that developed composite reversibly absorb hydrogen at 350 °C similar to Mg. The absorption kinetics increased with increase in fold and rolling operation. Finer dispersion of Ti and SS serves as heterogeneous nucleation sites for MgH_2 and forms shorter diffusion paths with more dislocation networks that increase hydrogen kinetics. ARB is also used to process Mg-LaNi5-Soot by Mohammad Faisal et al. [104] to improve the hydrogen storage capacity. It was observed that hydrogen kinetics increased due to refined nanoscale features and abundant heterogeneous interfaces. Presence of both LaNi5 and Soot in Mg-Mg interface act as nucleation sites for MgH_2. Increase in ARB process decreases the particle size of LaNi5 up to 60 nm and also induces the micro strain and decreases the plateau pressure thus sorption behaviour increases. Addition of these particles increases the hydrogen storage capacity of Mg up to 4.5 wt% and JMAK analysis confirms diffusion controlled 2D growth mechanism in MgH_2 nuclei. Anshul Gupta et al. [105] used ARB method to improve the hydrogen storage capacity of Mg–Mg_2Ni--graphite composite. ARB processed composite exhibited 5.9 wt%

storage capacity with significant improvement in desorption kinetics. Usage of these reinforcements results in formation of Mg_2NiH_4 and MgH_2 phases that decrease the activation energy. ARB induces hydrogen release by facilitating large interfacial area and defect density in Mg_2Ni phase that acts as the nucleation sites to accelerate hydrogen release. Laminated Mg-Cu composites are developed by ARB approach to initiates hydrogenation. Formation of form Mg_2Cu layers was observed at lower temperature due the reduction in activation energy with high defect in lattice density. Also, it was depicted that SPD method improves the atomic diffusion that enable quick formation of Mg_2Cu phase even in presence of MgO [106]. Cold rolling is also coupled with various process such HEBM, ECAP and rolling to develop porous structured Mg composite with improved hydrogen storage capacity.

Roozbeh Parviz et al. [107] developed porous layered Mg–Ni–Mo–C composite by combing HEBM, ECAP, cold rolling and subsequent heat treatment (Fig. 7). The metal powders were first ball milled and then processed by ECAP and cold rolling, followed by heat treatment at 450 °C for 5 h. This combined process forms Mg_2Ni intermetallic, NiO and MgO catalyst that enhances the hydrogen kinetics and decreases the activation energy. The porous oxide network between Mg layers significantly improved H_2 diffusion and mechanical stability during cycling. Also, it was observed that the adopted process uniformly dispersed in-situ catalysts that significantly enhances hydrogen sorption kinetics and structural stability. The synergy of ECAP, rolling and heat treatment lowers desorption temperature and activation energy making it ideal for practical H_2 storage applications [108].

H. Vafaeenezhad et al. [109] combined the radial axial ring rolling technique and hot upsetting process (Fig. 8a-b) to improve the hydrogen storage behaviour of Mg–3Zn–1Ca-0.5Mn alloy. Initially. cylindrical billets were hot-upset at 400 °C using a 1000-ton press and then pierced and ring-rolled at 430 °C using a radial-axial ring rolling mill. Observation revealed significant grain refinement and dislocation substructures with improved hydrogen absorption up to 10 wt% in 30 min and enhanced desorption of 6 wt% in 20 min. This improvement is attributed to SPD process that refined grains and effective interfaces that facilitate hydrogen diffusion.

4.4. Forging and Friction stir processing

Forging is an SPD method that reduces material height by applying compression and heating that promotes fine grain refinement and accelerate hydrogen kinetics. Various forging method are adopted by researchers such as fast forging, accumulative fold forging and swaging to attain finer grain refinement. Patricia de Rango et al. [110] adopted fast forging to improve the hydrogen kinetics of Mg-Ni alloys. Mg and Nickel powders are compacted and closed in metal sheath and hammer of 150 Kg is dropped on the sample to create deformation. Results revealed that fast forging induces fine grain refinement and defects at low temperate and forms Mg_2Ni phase at high temperate. Also, it was observed the faster kinetics are achieved for fast forged samples while compared with ball milled sample. Accumulative fold forging is adopted by F. Khodabakhshi et al. [111]to develop nanostructured Mg/Ni layered composite. Herein Mg powders are folded in nickel foil with 1:1 and 2:1 ratio and compressed with 50 % reduction in thickness. The procedure is repeated for 20 cycles that generates 1048,576 nanolayer and the grain size of Mg and Ni are reduced to ~900 nm and ~400 nm wherein improvement in hydrogen kinetics is achieved at 623–873 K under 5 MPa. Mg-9.1Y-1.8Zn alloys are subjected to extrusion followed by swaging process to improve hydrogen storage properties. S.X. Pan et al. [112] observed the breaking down of LPSO phases during hydrogenation and also depicted that swaging process refines the grains in the range of 80–200 nm. Furthermore, it induces the nanocrystals formation that improve the hydrogen diffusion and increases the kinetics. Swages alloy exhibits higher absorption capacity of 6.58 % due to the in-situ formed hydride which acts as catalyst and improves the performance.

FS) is a low-cost method used to improve the hydrogen kinetics of Mg alloy by promoting finer grain refinement and also helps in uniform dispersion of formed intermetallic phases. E.P. Silva et al. [113] performed FSP on ZK60 alloy to improve its hydrogen storage capacity. It was observed that FSP promotes ultrafine grain refinement and chips taken from stir zone exhibits higher absorption of 6.3 wt% in 24 hr and rapid desorption owing to thinner intermetallic layer and higher surface area. Furthermore, it was depicted that increase in FSP cycles increases hydrogen storage kinetics. Same research group stir casted ZK60 alloy with 1.5 wt% mischmetal [114] and performed FSP on the developed alloy. It was observed that FSP induces grain refinement, breaking of intermetallic phases, dynamic recrystallization and increase grain boundaries density (Fig. 9a-c) that acts as diffusion path for hydrogen. FSP process results in 24 % increment in hydrogen absorption and casted alloy exhibits 3.8 min hydrogen desorption while FSPed alloy has

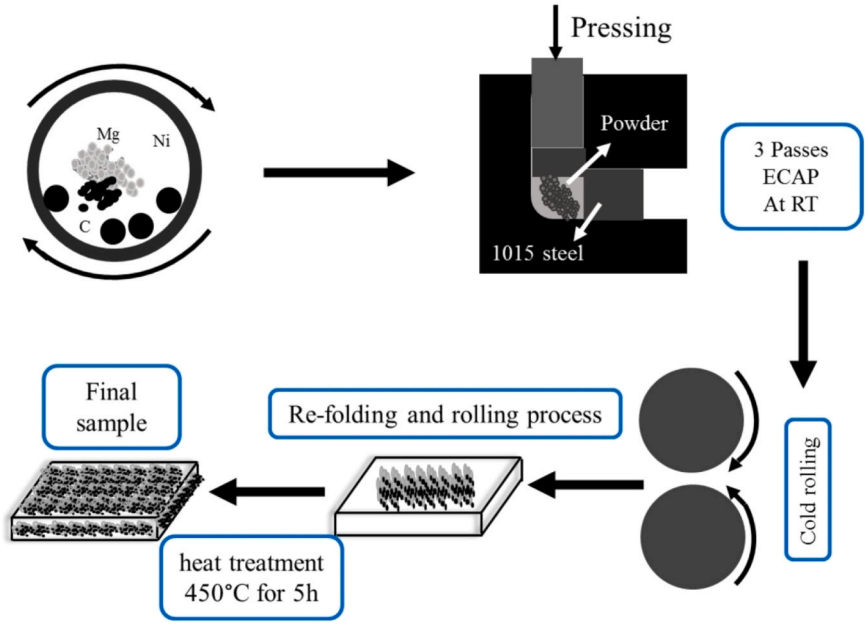

Fig. 7. representation of combined SPD method [107].

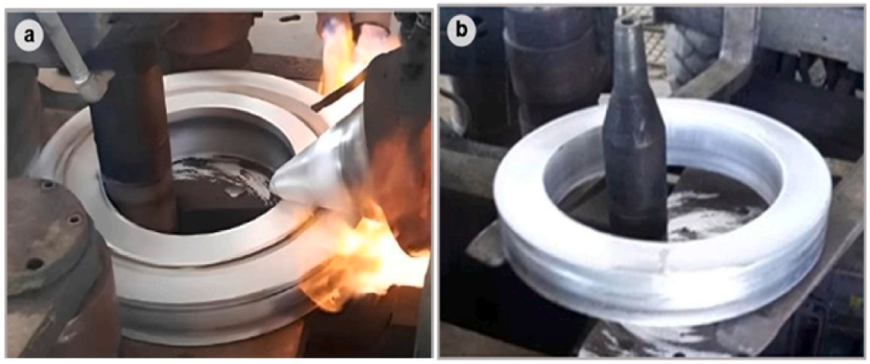

Fig. 8. a) Deformation in ring rolled alloy b) SPD proceed alloy [109].

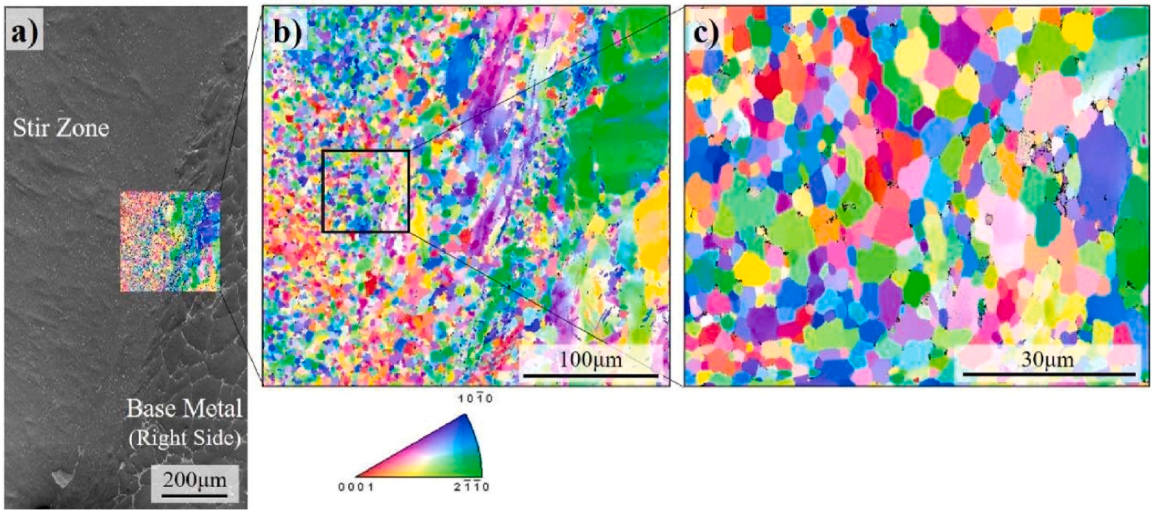

Fig. 9. Stir zone of ZK60-Mm alloy a) SE mode b) inverse pole figure c) enlarged image of b. [114].

1.9 min desorption of hydrogen.

Bin Li et al. [115] used cold rolling and FSP method on Mg-*x*Mn-0.5Al to understand its hydrogen storage mechanism. It was observed that incorporation of Mn and Al increases the dislocation density and forms Al8Mn5 and α-Mn phases. FSP process fragments the α-Mn particles and increases its surface area which increases its catalytic activity. Cold rolling generates elongated grain and secondary phases that increases the hydrogen kinetics. The processed alloy exhibited rapid absorption of hydrogen with 5 wt% in 3 min at 623 K and decreases activation energy to ~125 kJ/mol. Molecular sieve reinforced Mg-Li composite also developed through FSP process and the outline of fabrication process is depicted in Fig. 10 (a-b). It was observed that addition of reinforcement increases the reversible capacity up to 6 wt%. FSP initiates lattice defects and presence of reinforcement increase the

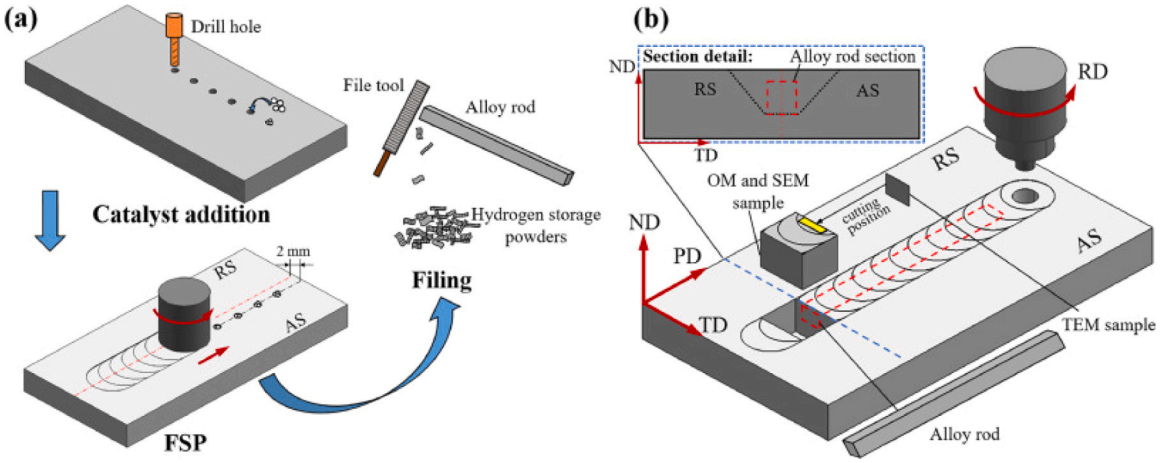

Fig. 10. Representation of FSP process a) preparation of sample b) sectional view of sample [116].

dislocation and grain boundaries that accelerated the hydrogen diffusion kinetic. FSP induces heterogeneous nucleation sites that decrease the activation energy [116].

SPD process significantly increases the kinetics of hydrogen storage in Mg and its alloys by inducing fine grained microstructure and generates high density of crystal lattice defects viz. grain boundaries and dislocations. These defects generate faster diffusion pathways that facilitate the hydrogen desorption and absorption kinetics that increase the activation kinetics under normal conditions while compared to other conventional techniques.

Unlike ball milling, SPD approach can form bulk materials with air resistant and minimal prone to oxidation that helps in safer and easier handling. Techniques like ECAP, HPT, ARB and FSP will consolidate the powders into dense forms, additionally enhances the cycling stability and sorption rates of hydrogen. FSP generates fine grained microstructures with stable secondary phase that act as the active nucleation sites which improves hydrogen kinetic. SPD also interrupts surface oxide layers that act as active catalytic sites which help in rapid hydrogen uptake. Furthermore, SPD has unique capability to activate Mg based materials by modifying both hydrogen interaction kinetics and thermodynamics that increase the wide spread application of Mg alloy in hydrogen storage systems.

5. Conclusion and perspective

This review systemically explored the hydrogen storage ability of Mg and its alloys that includes hydrogen storage mechanism, influence of varying alloying elements and reinforcement in Mg, various processing method to improve its hydrogen kinetics. 2 deals with hydrogen storage mechanisms in Mg alloy system such as stability, hydrogenation and dehydrogenation behaviour and various mechanism are elaborated. 3 delivers effect of various alloying elements and reinforcement on hydrogen storage behaviour of Mg alloy. 4 explained the detailed studies related to SPD of Mg alloy on hydrogen kinetic. Still serval issues should be focused on future research to improve the properties and application of Mg alloy in hydrogen storage. SPD method alters the thermodynamics of Mg alloy in hydrogen systems and plays vital role in enhancing the hydrogen kinetics. When compared to conventional ball milling approach SPD increases the dislocations, grain boundaries and reduces the activation energy. However, to date, scalability of the process for larger volume production has not been focused to commercialize the industrial scale production for ultrafine grained Mg based hydrogen storage materials. High processing loads, long processing times and specialized tooling increases the overall cost. Additionally, grain refinement achieved by SPD may suffer from thermal instability during prolonged hydrogenation/dehydrogenation cycling, leading to coarsening and performance degradation. Controlling uniform grain size across bulk samples and avoiding contamination during processing are further challenges. Further studies should focus on atomic scale hydrogen diffusion and the interaction between alloying elements or reinforcement. Optimization in microstructure will help to improve performance of Mg alloy in hydrogen storage. Heat transfer behaviour in deformed structures is still underexplored. Enhancing cycling stability and combining catalysts with SPD could further improve low-temperature kinetics. Most importantly, integrating thermodynamic modelling with experiments is essential for developing next-generation materials for practical hydrogen applications.

Author contribution

Every author has equal contribution.

CRediT authorship contribution statement

All authors have equally contributed.

Ethical approval

Not applicable.

Declaration of Competing Interest

The authors declare that they have no known competing financial interests or personal relationships that could have appeared to influence the work reported in this paper.

Data Availability

Not applicable

References

[1] T.K. Pani, S. Muduli, K.K. Garlapati, S.K. Martha, V2O5-MnO2 nanocomposites as an efficient electrode material for high-performance aqueous supercapacitors, Mater. Today Sustain. 28 (2024) 101010, https://doi.org/10.1016/j.mtsust.2024.101010.
[2] M. Tomy, A. Ambika Rajappan, V. VM, X. Thankappan Suryabai, Emergence of Novel 2D materials for high-performance supercapacitor electrode applications: a brief review, Energy Fuels 35 (2021) 19881–19900, https://doi.org/10.1021/acs.energyfuels.1c02743.
[3] L. Montero de Espinosa, W. Meesorn, D. Moatsou, C. Weder, Bioinspired polymer systems with stimuli-responsive mechanical properties, Chem. Rev. 117 (2017) 12851–12892.
[4] Y. Li, D. Pan, J. Cao, W. Fang, Y. Bao, B. Liu, Recent advances in high-entropy ceramics: design principles, structural characteristics, and emerging properties, Extrem. Mater. 1 (2025) 42–72, https://doi.org/10.1016/j.exm.2025.05.002.
[5] P. Jiao, J. Mueller, J.R. Raney, X. Zheng, A.H. Alavi, Mechanical metamaterials and beyond, Nat. Commun. 14 (2023) 6004.
[6] A.S. Mekonnin, K. Wacławiak, M. Humayun, S. Zhang, H. Ullah, Hydrogen storage technology, and its challenges: a review, Catalysts 15 (2025) 260.
[7] A. Züttel, A. Remhof, A. Borgschulte, O. Friedrichs, Hydrogen: the future energy carrier, Philos. Trans. R. Soc. A Math. Phys. Eng. Sci. 368 (2010) 3329–3342.
[8] L. Schlapbach, A. Züttel, Hydrogen-storage materials for mobile applications, Nature 414 (2001) 353–358.
[9] Y. Shang, C. Pistidda, G. Gizer, T. Klassen, M. Dornheim, Mg-based materials for hydrogen storage, J. Magnes. Alloy. 9 (2021) 1837–1860, https://doi.org/10.1016/j.jma.2021.06.007.
[10] A. Züttel, Materials for hydrogen storage, Mater. Today 6 (2003) 24–33.
[11] K. Mazloomi, C. Gomes, Hydrogen as an energy carrier: prospects and challenges, Renew. Sustain. Energy Rev. 16 (2012) 3024–3033.
[12] J.O. Jensen, A.P. Vestbø, Q. Li, N.J. Bjerrum, The energy efficiency of onboard hydrogen storage, J. Alloy. Compd. 446 (2007) 723–728.
[13] M. Klell, Handbook of hydrogen storage. Storage of Hydrogen in the Pure Form, 2010.
[14] C.W. Hamilton, R.T. Baker, A. Staubitz, I. Manners, B–N compounds for chemical hydrogen storage, Chem. Soc. Rev. 38 (2009) 279–293.
[15] J. Ren, N.M. Musyoka, H.W. Langmi, M. Mathe, S. Liao, Current research trends and perspectives on materials-based hydrogen storage solutions: a critical review, Int J. Hydrog. Energy 42 (2017) 289–311.
[16] L. Shao, X. Lin, X. Yang, Y. Zhao, J. Zhang, T. Cheng, et al., Magnesium-based hydrogen storage tanks: a review of research, development and simulation models, Renew. Sustain. Energy Rev. 211 (2025) 115332, https://doi.org/10.1016/j.rser.2025.115332.
[17] Z.-Y. Dai, P. Wu, L.-R. Xiao, H. Kimura, C.-X. Hou, X.-Q. Sun, et al., Non-stoichiometric Ni3ZnC0.7 carbide loading on melamine sponge-derived carbon for hydrogen storage performance improvement of MgH2, Rare Met. 44 (2025) 515–530, https://doi.org/10.1007/s12598-024-02943-y.
[18] B. Zhang, X. Xie, Y. Wang, C. Hou, X. Sun, Y. Zhang, et al., In situ formation of multiple catalysts for enhancing the hydrogen storage of MgH2 by adding porous Ni3ZnC0.7/Ni loaded carbon nanotubes microspheres, J. Magnes. Alloy. 12 (2024) 1227–1238, https://doi.org/10.1016/j.jma.2022.07.004.
[19] Q. Li, Y. Lu, Q. Luo, X. Yang, Y. Yang, J. Tan, et al., Thermodynamics and kinetics of hydriding and dehydriding reactions in Mg-based hydrogen storage materials, J. Magnes. Alloy. 9 (2021) 1922–1941.
[20] M. Paskevicius, D.A. Sheppard, C.E. Buckley, Thermodynamic changes in mechanochemically synthesized magnesium hydride nanoparticles, J. Am. Chem. Soc. 132 (2010) 5077–5083.
[21] S. Dong, C. Li, J. Wang, H. Liu, Z. Ding, Z. Gao, et al., The “burst effect” of hydrogen desorption in MgH 2 dehydrogenation, J. Mater. Chem. A Mater. 10 (2022) 22363–22372.
[22] C. Zhou, Y. Peng, Q. Zhang, Growth kinetics of MgH2 nanocrystallites prepared by ball milling, J. Mater. Sci. Technol. 50 (2020) 178–183.
[23] L. Ouyang, Z. Cao, H. Wang, R. Hu, M. Zhu, Application of dielectric barrier discharge plasma-assisted milling in energy storage materials–a review, J. Alloy. Compd. 691 (2017) 422–435.
[24] F.J. Desai, M.N. Uddin, M.M. Rahman, R. Asmatulu, A critical review on improving hydrogen storage properties of metal hydride via nanostructuring and

integrating carbonaceous materials, Int J. Hydrog. Energy 48 (2023) 29256–29294.
[25] D.R. Leiva, A.M. Jorge, T.T. Ishikawa, J. Huot, D. Fruchart, S. Miraglia, et al., Nanoscale grain refinement and H-sorption properties of MgH2 processed by high-pressure torsion and other mechanical routes, Adv. Eng. Mater. 12 (2010) 786–792.
[26] L. Ren, Y. Li, N. Zhang, Z. Li, X. Lin, W. Zhu, et al., Nanostructuring of Mg-based hydrogen storage materials: recent advances for promoting key applications, Nanomicro Lett. 15 (2023) 93.
[27] R. Bardhan, A.M. Ruminski, A. Brand, J.J. Urban, Magnesium nanocrystal-polymer composites: a new platform for designer hydrogen storage materials, Energy Environ. Sci. 4 (2011) 4882–4895.
[28] M. Paskevicius, D.A. Sheppard, C.E. Buckley, Thermodynamic changes in mechanochemically synthesized magnesium hydride nanoparticles, J. Am. Chem. Soc. 132 (2010) 5077–5083.
[29] A.S. Pedersen, J. Kjøller, B. Larsen, B. Vigeholm, Magnesium for hydrogen storage, Int J. Hydrog. Energy 8 (1983) 205–211.
[30] J. Huot, G. Liang, S. Boily, A. Van Neste, R. Schulz, Structural study and hydrogen sorption kinetics of ball-milled magnesium hydride, J. Alloy. Compd. 293 (1999) 495–500.
[31] J.F. Fernandez, C.R. Sanchez, Rate determining step in the absorption and desorption of hydrogen by magnesium, J. Alloy. Compd. 340 (2002) 189–198.
[32] T.R. Jensen, A. Andreasen, T. Vegge, J.W. Andreasen, K. Ståhl, A.S. Pedersen, et al., Dehydrogenation kinetics of pure and nickel-doped magnesium hydride investigated by in situ time-resolved powder X-ray diffraction, Int J. Hydrog. Energy 31 (2006) 2052–2062.
[33] M. Pezat, B. Darriet, P. Hagenmuller, A comparative study of magnesium-rich rare-earth-based alloys for hydrogen storage, J. Less Common Met. 74 (1980) 427–434.
[34] P. Spatz, H.A. Aebischer, A. Krozer, L. Schlapbach, The diffusion of H in Mg and the nucleation and growth of MgH2 in thin films, Z. Phys. Chem. 181 (1993) 393–397.
[35] H.T. Uchida, S. Wagner, M. Hamm, J. Kürschner, R. Kirchheim, B. Hjörvarsson, et al., Absorption kinetics and hydride formation in magnesium films: Effect of driving force revisited, Acta Mater. 85 (2015) 279–289.
[36] V.A. Yartys, M.V. Lototskyy, E. Akiba, R. Albert, V.E. Antonov, J.-R. Ares, et al., Magnesium based materials for hydrogen based energy storage: past, present and future, Int J. Hydrog. Energy 44 (2019) 7809–7859.
[37] A. Gupta, G.V. Baron, P. Perreault, S. Lenaerts, R.-G. Ciocarlan, P. Cool, et al., Hydrogen clathrates: next generation hydrogen storage materials, Energy Storage Mater. 41 (2021) 69–107.
[38] R.W.P. Wagemans, J.H. van Lenthe, P.E. de Jongh, A.J. van Dillen, K.P. de Jong, Hydrogen storage in magnesium clusters: quantum chemical study, J. Am. Chem. Soc. 127 (2005) 16675–16680.
[39] Y. Fu, L. Zhang, Y. Li, S. Guo, Z. Yu, W. Wang, et al., Catalytic effect of MOF-derived transition metal catalyst FeCoS@ C on hydrogen storage of magnesium, J. Mater. Sci. Technol. 138 (2023) 59–69.
[40] M. Felderhoff, B. Bogdanović, High temperature metal hydrides as heat storage materials for solar and related applications, Int. J. Mol. Sci. 10 (2009) 325–344.
[41] P. Martino, M. Chiesa, M.C. Paganini, E. Giamello, Coadsorption of NO and H2 at the surface of MgO monitored by EPR spectroscopy. Towards a site specific discrimination of polycrystalline oxide surfaces, Surf. Sci. 527 (2003) 80–88.
[42] A.S. Pedersen, B. Vigeholm, J. Kjøller, B. Larsen, The effect of cycling in impure hydrogen on the hydrogen capacity of magnesium powder, Int J. Hydrog. Energy 12 (1987) 765–771.
[43] P. Hjort, A. Krozer, B. Kasemo, Hydrogen sorption kinetics in partly oxidized Mg films, J. Alloy. Compd. 237 (1996) 74–80.
[44] E. Xu, H. Li, X. You, C. Bu, L. Zhang, Q. Wang, et al., Influence of micro-amount O2 or N2 on the hydrogenation/dehydrogenation kinetics of hydrogen-storage material MgH2, Int. J. Hydrog. Energy 42 (2017) 8057–8062.
[45] E. Xu, H. Li, X. You, C. Bu, L. Zhang, Q. Wang, et al., Influence of micro-amount O2 or N2 on the hydrogenation/dehydrogenation kinetics of hydrogen-storage material MgH2, Int. J. Hydrog. Energy 42 (2017) 8057–8062, https://doi.org/10.1016/j.ijhydene.2016.12.102.
[46] F. Sun, M. Yan, X. Liu, J. Ye, Z. Li, S. Wang, et al., Effect of N2, CH4 and O2 on hydrogen storage performance of 2LiNH2 + MgH2 system, Int. J. Hydrog. Energy 40 (2015) 6173–6179, https://doi.org/10.1016/j.ijhydene.2015.03.084.
[47] X.Q. Tran, S.D. McDonald, Q. Gu, X.F. Tan, K. Nogita, Effect of impurity N2 concentration on the hydriding kinetics of Na-doped Mg–Ni alloys, Int. J. Hydrog. Energy 42 (2017) 366–375, https://doi.org/10.1016/j.ijhydene.2016.08.110.
[48] Y. Xinglin, L. Xiaohui, Z. Jiaqi, H. Quanhui, Z. Junhu, Progress in improving hydrogen storage properties of Mg-based materials, Mater. Today Adv. 19 (2023) 100387.
[49] X. Liu, S. Wu, X. Cai, L. Zhou, Hydrogen storage behaviour of Cr-and Mn-doped Mg2Ni alloys fabricated via high-energy ball milling, Int. J. Hydrog. Energy 48 (2023) 17202–17215.
[50] H. Imamura, K. Yoshihara, M. Yoo, I. Kitazawa, Y. Sakata, S. Ooshima, Dehydriding of Sn/MgH2 nanocomposite formed by ball milling of MgH2 with Sn, Int. J. Hydrog. Energy 32 (2007) 4191–4194.
[51] J.J. Vajo, F. Mertens, C.C. Ahn, Jr.R.C. Bowman, B. Fultz, Altering hydrogen storage properties by hydride destabilization through alloy formation: LiH and MgH2 destabilized with Si, J. Phys. Chem. B 108 (2004) 13977–13983.
[52] G.S. Walker, M. Abbas, D.M. Grant, C. Udeh, Destabilisation of magnesium hydride by germanium as a new potential multicomponent hydrogen storage system, Chem. Commun. 47 (2011) 8001–8003.
[53] H.C. Zhong, H. Wang, L.Z. Ouyang, Improving the hydrogen storage properties of MgH2 by reversibly forming Mg–Al solid solution alloys, Int. J. Hydrog. Energy 39 (2014) 3320–3326.
[54] B. Boruah, B. Kalita, Alloying ratio versus cluster size for reversible hydrogen storage in 3d transition metal doped small Mg clusters: dispersion corrected DFT study, J. Energy Storage 72 (2023) 108217.
[55] Jr.J.J. Reilly, Jr.R.H. Wiswall, Reaction of hydrogen with alloys of magnesium and nickel and the formation of Mg2NiH4, Inorg. Chem. 7 (1968) 2254–2256.
[56] J.-C. Crivello, V. Denys R, M. Dornheim, M. Felderhoff, D.M. Grant, J. Huot, et al., Mg-based compounds for hydrogen and energy storage, Appl. Phys. A 122 (2016) 1–17.
[57] Y. Xu, Y. Zhou, Y. Li, Y. Hao, P. Wu, Z. Ding, Magnesium-based hydrogen storage alloys: advances, strategies, and future outlook for clean energy applications, Molecules 29 (2024) 2525.
[58] Jr.J.J. Reilly, Jr.R.H. Wiswall, Reaction of hydrogen with alloys of magnesium and copper, Inorg. Chem. 6 (1967) 2220–2223.
[59] X. Zhang, R. Yang, J. Qu, W. Zhao, L. Xie, W. Tian, et al., The synthesis and hydrogen storage properties of pure nanostructuredMg2FeH6, Nanotechnology 21 (2010) 095706.
[60] E. Callini, L. Pasquini, L.H. Rude, T.K. Nielsen, T.R. Jensen, E. Bonetti, Hydrogen storage and phase transformations in Mg–Pd nanoparticles, J. Appl. Phys. 108 (2010).
[61] H. Oesterreicher, H. Bittner, Hydride formation in La1− xMgxNi2, J. Less Common Met. 73 (1980) 339–344.
[62] X. Li, Y. Fu, Y. Xie, L. Cong, H. Yu, L. Zhang, et al., Effect of Ni/tubular g-C3N4 on hydrogen storage properties of MgH2, Int. J. Hydrog. Energy 46 (2021) 33186–33196.
[63] Z. Yuan, S. Li, K. Wang, N. Xu, W. Sun, L. Sun, et al., In-situ formed Pt nano-clusters serving as destabilization-catalysis bi-functional additive for MgH2, Chem. Eng. J. 435 (2022) 135050.
[64] L.-R. Xiao, C. Chen, S. Wang, Z.-Y. Dai, H. Kimura, C. Ni, et al., Effects of Ti- and Nb-based transition element from single to multiple compound oxides and carbon-based composite additives on Mg-MgH2 hydrogen storage material, Tungsten 7 (2025) 32–49, https://doi.org/10.1007/s42864-024-00287-9.
[65] H. Torabi, S.M. Hosseini, A. Siahsarani, A. Najafi, A. Masoumi, G. Faraji, Processing of different Mg-based multiphase alloys via a combined severe plastic deformation, Mater. Sci. Technol. 40 (2024) 236–246.
[66] V. Ponnusamy, N. Kumar, Effect of rolling on microstructure and mechanical properties of dual phase Mg–8Li–graphene composite, World J. Eng. 22 (2025) 725–733.
[67] C.-R. Song, S.-Y. Zhang, L. Liu, H.-Y. Yang, J. Kang, J. Meng, et al., Research progress on the microstructure evolution mechanisms of al-Mg alloys by severe plastic deformation, Materials 17 (2024) 4235.
[68] S.A. Paranjape, T.G. Nikhil, S. Suwas, L.S. Toth, S.V. Kailas, Comparison of microstructure and texture in pure magnesium sheets produced by hot rolling and a new SPD process; the high-pressure compressive reciprocating shear, Mater. Charact. 225 (2025) 115209, https://doi.org/10.1016/j.matchar.2025.115209.
[69] C.C. Li, R.E. Kim, X.G. Qiao, W.T. Sun, L. Yuan, H.S. Kim, et al., Achieving exceptional room-temperature ductility in ultrafine-grained Mg-0.8 Mn alloy via high pressure torsion, J. Alloy. Compd. 1020 (2025) 179411.
[70] M. Li, M. Yao, Y. Ning, J. Yu, Z. Xing, S. Gao, et al., The effects of ECAP, Mn and Ca elements on the microstructure and corrosion properties of magnesium alloys were investigated, Int. J. Electrochem Sci. 19 (2024) 100850.
[71] Z. Zheng, Q. Li, X. Chen, A. Gao, N. Zhang, Application status and prospects of friction stir processing in wrought magnesium alloys: a review, Trans. Indian Inst. Met. 77 (2024) 1891–1906, https://doi.org/10.1007/s12666-024-03290-3.
[72] V.M. Skripnyuk, E. Rabkin, Y. Estrin, R. Lapovok, The effect of ball milling and equal channel angular pressing on the hydrogen absorption/desorption properties of Mg–4.95 wt% Zn–0.71 wt% Zr (ZK60) alloy, Acta Mater. 52 (2004) 405–414.
[73] J. Huot, N.Ye Skryabina, D. Fruchart, Application of severe plastic deformation techniques to magnesium for enhanced hydrogen sorption properties, Metals 2 (2012) 329–343, https://doi.org/10.3390/met2030329.
[74] S.-J. Huang, C. Chiu, T.-Y. Chou, E. Rabkin, Effect of equal channel angular pressing (ECAP) on hydrogen storage properties of commercial magnesium alloy AZ61, Int. J. Hydrog. Energy 43 (2018) 4371–4380, https://doi.org/10.1016/j.ijhydene.2018.01.044.
[75] N. Skryabina, N. Medvedeva, A. Gabov, D. Fruchart, S. Nachev, P. de Rango, Impact of severe plastic deformation on the stability of MgH2, J. Alloy. Compd. 645 (2015) S14–S17, https://doi.org/10.1016/j.jallcom.2015.03.128.
[76] V. Skripnyuk, E. Buchman, E. Rabkin, Y. Estrin, M. Popov, S. Jorgensen, The effect of equal channel angular pressing on hydrogen storage properties of a eutectic Mg–Ni alloy, J. Alloy. Compd. 436 (2007) 99–106, https://doi.org/10.1016/j.jallcom.2006.07.030.
[77] W.B. Silva, D.R. Leiva, R. Floriano, L.E.R. Vega, V.B. Oliveira, J. Gallego, et al., Magnesium alloys for hydrogen storage processed by ECAP followed by low temperature rolling, Mater. Res. 25 (2022) e20210214.
[78] L. Wang, J. Jiang, A. Ma, Y. Li, D. Song, A critical review of mg-based hydrogen storage materials processed by equal channel angular pressing, Metals 7 (2017), https://doi.org/10.3390/met7090324.
[79] A.M. Jorge Jr, E. Prokofiev, M.R.M. Triques, V. Roche, W.J. Botta, C.S. Kiminami, et al., Effect of cold rolling on the structure and hydrogen properties of AZ91 and AM60D magnesium alloys processed by ECAP, Int. J. Hydrog. Energy 42 (2017) 21822–21831, https://doi.org/10.1016/j.ijhydene.2017.07.118.
[80] J. Soyama, R. Floriano, D.R. Leiva, Y. Guo, A.M. Jorge Junior, E. Pereira da Silva, et al., Severely deformed ZK60 + 2.5% Mm alloy for hydrogen storage produced

by two different processing routes, Int. J. Hydrog. Energy 41 (2016) 11284–11292, https://doi.org/10.1016/j.ijhydene.2016.05.031.
[81] A.A.C. Asselli, D.R. Leiva, J. Huot, M. Kawasaki, T.G. Langdon, W.J. Botta, Effects of equal-channel angular pressing and accumulative roll-bonding on hydrogen storage properties of a commercial ZK60 magnesium alloy, Int. J. Hydrog. Energy 40 (2015) 16971–16976, https://doi.org/10.1016/j.ijhydene.2015.05.149.
[82] S.-J. Huang, V. Rajagopal, Y.L. Chen, Y.-H. Chiu, Improving the hydrogenation properties of AZ31-Mg alloys with different carbonaceous additives by high energy ball milling (HEBM) and equal channel angular pressing (ECAP), Int. J. Hydrog. Energy 45 (2020) 22291–22301, https://doi.org/10.1016/j.ijhydene.2019.10.032.
[83] S.-J. Huang, V. Rajagopal, A.N. Ali, Influence of the ECAP and HEBM processes and the addition of Ni catalyst on the hydrogen storage properties of AZ31-x Ni (x=0,2,4) alloy, Int. J. Hydrog. Energy 44 (2019) 1047–1058, https://doi.org/10.1016/j.ijhydene.2018.11.005.
[84] S.-J. Huang, M.P. Mose, V. Rajagopal, Effect of microstructure on the hydrogenation behavior of AZ61 magnesium alloy with silicon carbide and nickel additives, processed by equal channel angular pressing, Int. J. Hydrog. Energy 46 (2021) 4211–4221, https://doi.org/10.1016/j.ijhydene.2020.10.217.
[85] A. Abbas, Z.-B. Lin, R.-L. Ma, K.-M. Lin, H.-C. Lin, Effects of CNTs, graphene, and organic additives on hydrogen storage performance of severely deformed ZK60 alloy, Int. J. Hydrog. Energy 52 (2024) 1175–1184, https://doi.org/10.1016/j.ijhydene.2022.07.112.
[86] K. Edalati, K. Kitabayashi, Y. Ikeda, J. Matsuda, H.-W. Li, I. Tanaka, et al., Bulk nanocrystalline gamma magnesium hydride with low dehydrogenation temperature stabilized by plastic straining via high-pressure torsion, Scr. Mater. 157 (2018) 54–57.
[87] K. Edalati, A. Yamamoto, Z. Horita, T. Ishihara, High-pressure torsion of pure magnesium: Evolution of mechanical properties, microstructures and hydrogen storage capacity with equivalent strain, Scr. Mater. 64 (2011) 880–883, https://doi.org/10.1016/j.scriptamat.2011.01.023.
[88] K. Edalati, H. Emami, Y. Ikeda, H. Iwaoka, I. Tanaka, E. Akiba, et al., New nanostructured phases with reversible hydrogen storage capability in immiscible magnesium–zirconium system produced by high-pressure torsion, Acta Mater. 108 (2016) 293–303, https://doi.org/10.1016/j.actamat.2016.02.026.
[89] K. Edalati, H. Emami, A. Staykov, D.J. Smith, E. Akiba, Z. Horita, Formation of metastable phases in magnesium–titanium system by high-pressure torsion and their hydrogen storage performance, Acta Mater. 99 (2015) 150–156.
[90] T. Hongo, K. Edalati, M. Arita, J. Matsuda, E. Akiba, Z. Horita, Significance of grain boundaries and stacking faults on hydrogen storage properties of Mg2Ni intermetallics processed by high-pressure torsion, Acta Mater. 92 (2015) 46–54.
[91] S. Panda, J.-J. Fundenberger, Y. Zhao, J. Zou, L.S. Toth, T. Grosdidier, Effect of initial powder type on the hydrogen storage properties of high-pressure torsion consolidated Mg, Int. J. Hydrog. Energy 42 (2017) 22438–22448, https://doi.org/10.1016/j.ijhydene.2017.05.097.
[92] C. Xu, H.-J. Lin, K. Edalati, W. Li, L. Li, Y. Zhu, Superior hydrogenation properties in a Mg65Ce10Ni20Cu5 nanoglass processed by melt-spinning followed by high-pressure torsion, Scr. Mater. 152 (2018) 137–140, https://doi.org/10.1016/j.scriptamat.2018.04.036.
[93] M. Osorio-García, K. Suárez-Alcántara, Y. Todaka, A. Tejeda-Ochoa, M. Herrera-Ramírez, O. Hernández-Silva, et al., Low-temperature hydrogenation of Mg-Ni-Nb2O5 alloy processed by high-pressure torsion, J. Alloy. Compd. 878 (2021) 160309, https://doi.org/10.1016/j.jallcom.2021.160309.
[94] A. Grill, J. Horky, A. Panigrahi, G. Krexner, M. Zehetbauer, Long-term hydrogen storage in Mg and ZK60 after Severe Plastic Deformation, Int. J. Hydrog. Energy 40 (2015) 17144–17152, https://doi.org/10.1016/j.ijhydene.2015.05.145.
[95] P. Cengeri, Y. Kimoto, M. Janoska, Z. Abbasi, Y. Morisada, H. Fujii, et al., Long term hydrogen storage properties of ZK60 Mg-alloy as processed by different methods of SPD, J. Mater. Sci. 59 (2024) 5906–5922, https://doi.org/10.1007/s10853-024-09529-0.
[96] M. Gajdics, T. Spassov, V.K. Kis, E. Schafler, Á. Révész, Microstructural and morphological investigations on Mg-Nb2O5-CNT nanocomposites processed by high-pressure torsion for hydrogen storage applications, Int. J. Hydrog. Energy 45 (2020) 7917–7928, https://doi.org/10.1016/j.ijhydene.2019.06.165.
[97] S. Amira, J. Huot, Effect of cold rolling on hydrogen sorption properties of die-cast and as-cast magnesium alloys, J. Alloy. Compd. 520 (2012) 287–294, https://doi.org/10.1016/j.jallcom.2012.01.049.
[98] K. Tanaka, N. Takeichi, H. Tanaka, N. Kuriyama, T.T. Ueda, M. Tsukahara, et al., Investigation of micro-structural transition through disproportionation and recombination during hydrogenation and dehydrogenation in Mg/Cu super-laminates, J. Mater. Sci. 43 (2008) 3812–3816, https://doi.org/10.1007/s10853-007-2134-4.
[99] N. Takeichi, K. Tanaka, H. Tanaka, T.T. Ueda, Y. Kamiya, M. Tsukahara, et al., Hydrogen storage properties of Mg/Cu and Mg/Pd laminate composites and metallographic structure, 543–8, J. Alloy. Compd. (2007) 446–447, https://doi.org/10.1016/j.jallcom.2007.04.220.
[100] J.J. Márquez, J. Soyama, R. de Araujo Silva, D.R. Leiva, R. Floriano, T. T. Ishikawa, et al., Processing of MgH2 by extensive cold rolling under protective atmosphere, Int. J. Hydrog. Energy 42 (2017) 2201–2208, https://doi.org/10.1016/j.ijhydene.2016.10.056.
[101] J.J. Márquez, D.R. Leiva, R. Floriano, J. Soyama, W.B. Silva, T.T. Ishikawa, et al., Hydrogen storage in MgH2LaNi5 composites prepared by cold rolling under inert atmosphere, Int. J. Hydrog. Energy 43 (2018) 13348–13355, https://doi.org/10.1016/j.ijhydene.2018.05.067.
[102] R. Floriano, D.R. Leiva, S. Deledda, B.C. Hauback, W.J. Botta, Cold rolling of MgH2 powders containing different additives, Int. J. Hydrog. Energy 38 (2013) 16193–16198, https://doi.org/10.1016/j.ijhydene.2013.10.029.
[103] M. Danaie, C. Mauer, D. Mitlin, J. Huot, Hydrogen storage in bulk Mg–Ti and Mg–stainless steel multilayer composites synthesized via accumulative roll-bonding (ARB), Int. J. Hydrog. Energy 36 (2011) 3022–3036, https://doi.org/10.1016/j.ijhydene.2010.12.006.
[104] M. Faisal, K. Balani, A. Subramaniam, Cross-sectional TEM investigation of Mg-LaNi5-Soot hybrids for hydrogen storage, Int. J. Hydrog. Energy 46 (2021) 5507–5519, https://doi.org/10.1016/j.ijhydene.2020.11.134.
[105] A. Gupta, M. Faisal, S. Shervani, K. Balani, A. Subramaniam, Thermodynamic and microstructural basis for the fast hydrogenation kinetics in Mg–Mg2Ni-carbon hybrids, Int. J. Hydrog. Energy 45 (2020) 11632–11640, https://doi.org/10.1016/j.ijhydene.2020.02.037.
[106] K. Tanaka, D. Nishino, K. Hayashi, S. Ikeuchi, R. Kondo, H.T. Takeshita, Formation of Mg2Cu at low temperature in Mg/Cu super-laminate composites during initial hydrogenation, Int. J. Hydrog. Energy 42 (2017) 22502–22510, https://doi.org/10.1016/j.ijhydene.2017.02.193.
[107] R. Parviz, A. Heydarinia, M. Nili-Ahmadabadi, Enhanced hydrogen storage via in-situ formation of oxide, metallic and intermetallic catalysts in a Mg-based porous-layered composite, Int. J. Hydrog. Energy 111 (2025) 220–227, https://doi.org/10.1016/j.ijhydene.2025.02.287.
[108] R. Parviz, A. Heydarinia, M. Khosravi, M. Nili-Ahmadabadi, New Mg-based composite with layered-porous structure for enhanced hydrogen storage, J. Energy Storage 117 (2025) 116145, https://doi.org/10.1016/j.est.2025.116145.
[109] H. Vafaeenezhad, B. Nateq, M. Mahmoudi, M. Fesahat, S. Azizpour, Hydrogen storage of Mg–3Zn–1Ca-0.5Mn industrial scale magnesium ring processed by hot upsetting and radial axial ring rolling, Int. J. Hydrog. Energy 130 (2025) 440–451, https://doi.org/10.1016/j.ijhydene.2025.04.122.
[110] P. de Rango, D. Fruchart, V. Aptukov, N. Skryabina, Fast forging: a new SPD method to synthesize Mg-based alloys for hydrogen storage, Int. J. Hydrog. Energy 45 (2020) 7912–7916, https://doi.org/10.1016/j.ijhydene.2019.07.124.
[111] F. Khodabakhshi, O. Ekrt, M. Abdi, A.P. Gerlich, M. Mottaghi, R. Ebrahimi, et al., Hydrogen storage behavior of Mg/Ni layered nanostructured composite materials produced by accumulative fold-forging, Int. J. Hydrog. Energy 47 (2022) 1048–1062, https://doi.org/10.1016/j.ijhydene.2021.10.096.
[112] S.X. Pan, J. Zhang, X.J. Zhou, R.S. Jin, J.H. He, J.N. Chen, et al., Investigation on hydrogen storage properties of as-cast, extruded and swaged Mg–Y–Zn alloys, Int. J. Hydrog. Energy 47 (2022) 34545–34554, https://doi.org/10.1016/j.ijhydene.2022.08.036.
[113] E.P. Silva, D.R. Leiva, H.C. Pinto, R. Floriano, A.M. Neves, W.J. Botta, Effects of friction stir processing on hydrogen storage of ZK60 alloy, Int. J. Hydrog. Energy 43 (2018) 11085–11091, https://doi.org/10.1016/j.ijhydene.2018.04.209.
[114] E.P. Silva, G.N.L. Silva, D.C. Knupp, D.R. Leiva, I.N. Bastos, W.J. Botta, et al., Effect of the addition of 1.5 wt% of mischmetal in the ZK60 alloy processed by Friction Stir Process (FSP) followed by filing on the H-absorption/desorption kinetics, Int. J. Hydrog. Energy 50 (2024) 1542–1554, https://doi.org/10.1016/j.ijhydene.2023.10.062.
[115] B. Li, X. Peng, Y. Yang, G. Wei, Q. Li, Y. Chen, et al., Enhancement mechanism of low alloying (Mn, Al) and plastic deformation for hydrogen storage kinetics of Mg alloy, Sep Purif. Technol. 353 (2025) 128350, https://doi.org/10.1016/j.seppur.2024.128350.
[116] B. Li, X. Sun, H. Chen, Y. Yang, Q. Luo, X. Yang, et al., Enhancing Mg-Li alloy hydrogen storage kinetics by adding molecular sieve via friction stir processing, J. Mater. Sci. Technol. 180 (2024) 45–54, https://doi.org/10.1016/j.jmst.2023.04.051.